mathematics

MDPI

Article

Power-Law Nanofluid Flow over a Stretchable Surface Due to Gyrotactic Microorganisms

Hossam A. Nabwey [1,2,*], Waqar A. Khan [3], A. M. Rashad [4], Fazal Mabood [5] and Taha Salah [6]

[1] Department of Mathematics, College of Science and Humanities in Al-Kharj, Prince Sattam Bin Abdulaziz University, Al-Kharj 11942, Saudi Arabia
[2] Department of Basic Engineering Science, Faculty of Engineering, Menoufia University, Shebin El-Kom 32511, Egypt
[3] Department of Mechanical Engineering, College of Engineering, Prince Mohammad Bin Fahd University, Al Khobar 31952, Saudi Arabia
[4] Department of Mathematics, Faculty of Science, Aswan University, Aswan 81528, Egypt
[5] Department of Information Technology, Fanshawe College London, London, ON N5Y 5R6, Canada
[6] Basic and Applied Sciences Department, College of Engineering and Technology, Arab Academy for Science & Technology and Maritime Transport (AASTMT), Aswan Branch 81528, Egypt
* Correspondence: eng_hossam21@yahoo.com or h.mohamed@psau.edu.sa

Abstract: This study aims to learn more about how the flow of a power-law nanofluid's mixed bio-convective stagnation point flow approaching a stretchable surface behaves with the presence of a passively controlled boundary condition. The governing equations incorporate the motile bacterium and nanoparticles, and the current model includes Brownian motion and thermophoresis effects. The governing equations are transformed into ordinary differential equations, which are then numerically solved using the Runge–KuttaFehlberg (RKF) with the shooting technique. The controlling parameters are chosen as follows: the velocity ratio parameter, ε, is taken between 0.1 and 1.5; the mixed convection parameter, λ, is considered in the range 0–3; the buoyancy ratio parameter is considered in the range between 0.1 and 4; the bio-convection parameter, Rb, is taken in the range 0–1; nanofluid parameters are taken in the range 0.1–0.7; the bioconvection Schmidt number is considered in the range 0.1–3; the Prandtl number is taken between 1–4; and the Schmidt number is taken between 1 and 3. The Nusselt number, skin friction, and nanoparticle volume fraction profiles are shown graphically to observe the impact of several parameters under consideration. Both the Schmidt number and the Brownian motion parameter are shown to significantly increase the Sherwood number. Thermophoresis, however, has been proven to lower the Sherwood number. Furthermore, the bioconvection constant and Peclet number both help to slow down the rate of mass transfer. The presented theoretical investigation has a considerable role in engineering, where nanofluid flow is applied to organize a bioconvection process to develop power generation and mechanical energy. One of the more essential features of bioconvection is the aggregation of nanoparticles with motile microorganisms requested to augment the stability, heat, and mass transmission.

Keywords: Brownian; motion; nanofluids; thermophoresis; bio-convection; power-law fluid

MSC: 76D05; 76D10; 80A10; 80A19

Citation: Nabwey, H.A.; Khan, W.A.; Rashad, A.M.; Mabood, F.; Salah, T. Power-Law Nanofluid Flow over a Stretchable Surface Due to Gyrotactic Microorganisms. *Mathematics* **2022**, *10*, 3285. https://doi.org/10.3390/math10183285

Academic Editors: Camelia Petrescu and Valeriu David

Received: 24 July 2022
Accepted: 7 September 2022
Published: 9 September 2022

1. Introduction

The importance of nanofluids has been increasing with time, and investigators intend to study the behavior of nanofluids subjected to heat transfer systems. Nanofluids and their implications in the industrial sector have grown more because of their homogeneous nature in thermal conductivity and rudimentary heat transfer. Typical fluids such as propylene glycol, water, and ethylene glycol, among others, have poor heat transfer properties. Nanofluid, a homogenous solid–liquid mixture, is applied to enhance the thermal conductivity

of the base fluid. Choi [1] and Das et al. [2] exposed the most remarkable characteristic of nanofluids: thermal conductivity is dependent on temperature. Nanofluids are extensively used in energy and biomedical applications (nano-drug delivery, cancer therapeutics, and nano cryosurgery) [3–5]. Buongiorno [6] examined the effect of convective transport in nanofluid by observing the heat transfer properties of the Brownian motion and thermophoresis. Numerous studies are presented in the literature to demonstrate the uses of nanofluid in various fields [7–10].

The study of heat relocation in power-law (non-Newtonian) fluids has received significant attention because of its application in different branches of modern technologies, industries, and engineering like polymer-thickened oils, liquid crystals, polymeric suspensions, and physiological fluid mechanics. Furthermore, instances showing a diversity of non-Newtonian characteristics contain biological fluids, pharmaceutical formulations, toiletries, synthetic lubricants, cosmetics, paints, and foodstuffs (see Irvine and Karni [11]). Various models have been reported to analyze the non-Newtonian attitude toward fluids. Among these patterns, which are famous for following the empirical Ostwald–de Waele model, in which the shear stress varies according to a power function of the strain rate, gained much acceptance. The theoretical analysis of power-law fluid was first scrutinized by Schowalter [12] and Acrivos et al. [13]. Rashad et al. [14] examined the power-law nanofluid flow across a vertical cone in a porous medium. Later on, several studies were analyzed by many investigators [5,15–17].

Bioconvection occurs as the natural microbe swims upwards. Thus, the microorganism is denser than the base fluids. Because there are so many microbes on the upper surface of the foundation, it becomes weak. As a result, the bacteria decrease and promote bioconvection, and the microbes' return to swimming strengthens the process. This bacterial emigration into the water raises the temperature and mass transfer in the environment. Because of medical advancements, microscopic kinds have significantly contributed to the improvement in human life. Microorganisms are essential for life and it cannot exist without them. Decreasing the length of the cavities and the cell resistance enables the construction of continuum numerical patterns. It is often approved that the nanoparticles of concentration distribution are massive relative to the cell pivot. Bioconvection occurs as combined nanofluids are addressed using heat and mass conversion. Platt [18] further proposed the concept of bioconvection, which characterizes the micro-structural flow brought on by gradation density, in addition to motile gyro-tacticmicro-organisms. The first study of the bioconvection of gyro-tactic motile bacteria, including nanoparticles, was conducted by Kuznetsov and Avramenko [19]. Kuznetsov [20] presented key discoveries of nanofluidbioconvection in a horizontal porous layer, including both nanoparticles and gyro-tactic motile bacteria. Khan and coworkers [7,21–24] investigated the free convection of non-Newtonian nanofluid numerically down a vertical plate in a porous media. They considered that the medium contains gyrotactic microorganisms and that the temperature, nanoparticle concentration, and motile microbe density are all controlled in the plate.

The local Nusselt, Sherwood, and density numbers are found to be strongly influenced by nanofluid and bioconvection parameters. Additionally, they provided a mathematical model to examine the flow of a water-based nanofluid containing gyrotactic microorganisms around a truncated cone with a convective boundary condition at the surface. It has been discovered that, as a surface grows rougher, the densities of the mobile microorganisms, Sherwood number, Nusselt number, and skin friction all increase. Nabwey and collaborators [8–10] investigated the flow of a nanofluid containing gyrotactic bacteria over an isothermal cone surface in the presence of viscous dissipation and Joule heating. Consideration was given to the combined effects of a transverse magnetic field and Navier slip in the flow. They also considered mixed bioconvective flow on a vertical wedge in a Darcy porous media filled with a nanofluid that contains both nanoparticles and gyrotactic bacteria. To combine energy and concentration equations with passively controlled boundary conditions, the effects of thermophoresis and Brownian motion are considered. They found that the buoyancy ratio and magnetic field parameters increase the local skin

friction coefficient, Nusselt number, Sherwood number, and local density of the motile microorganism's number. Ishak et al. [25] analyzed the flow of a two-dimensional stagnation point of an incompressible viscous fluid near a steady mixed convection boundary layer flow across a stretching vertical sheet in its plane. For an aiding flow, they demonstrated that both the skin friction coefficient and the local Nusselt number increase with the buoyancy ratio; however, when the Prandtl number increases, only the local Nusselt number increases and the skin friction coefficient decreases.

However, the current study intends to close the knowledge gap regarding the mixed bioconvective stagnation point flow of a power-law nanofluid towards a stretchable surface. The nanofluid flow will be mathematically modeled using Buongiorno's two-component, including the Brownian movement and thermophoresis aspects. Moreover, modeling of the motile microorganism and nanoparticles is addressed in the governing equations.

2. Governing Equations

The present study considers the mixed bioconvection flow of a non-Newtonian power-law nanofluid having motile microorganisms and obeying the Ostwald–de Waele model [18] near the stagnation point at a heated stretchable vertical surface coinciding with the plane y = 0. The flow is confined to the region y > 0, where x and y are the cartesian coordinates. The model suggested by Buongiorno is utilized for the nanofluid attitude in which the influence of thermophoresis and Brownian movement is taken into consideration. The stretchable surface is maintained at a constant temperature Tw along with the constant density of motile microorganisms N_w. The ambient temperature, concentration, and motile microorganisms are symbolized as T∞, C∞, and N∞, respectively. It is considered that the stretching velocity is given by Uw(x) = cx and the velocity of external flow in the neighborhood of the stagnation point at x = y = 0 is given by U∞(x) = ax, where a and c are positive constants. Although, in the past, this reality is eliminated, in a practical situation, there is no nanoparticle flux on the boundaries, and the values of the nanofluid fraction C adapt to the concentration distribution. This means that we consider passively controlled boundary conditions as proposed by Kuznetsov and Nield [26].

Under the above-mentioned assumptions, the physical description of the problem under consideration in Figure 1 with Boussinesq approximations can be expressed as follows [8,24]:

$$\frac{\partial u}{\partial x} + \frac{\partial v}{\partial y} = 0 \tag{1}$$

$$u\frac{\partial u}{\partial x} + v\frac{\partial u}{\partial y} = U_\infty \frac{dU_\infty}{dx} + \frac{1}{\rho_f}\frac{\partial \tau_{xy}}{\partial y} + \frac{1}{\rho_f}\begin{bmatrix} (1-C_\infty)g\beta(T-T_\infty) \\ -(\rho_p-\rho_f)g(C-C_\infty) \\ -(\rho_m-\rho_f)g\gamma(N-N_\infty) \end{bmatrix} \tag{2}$$

$$u\frac{\partial T}{\partial x} + v\frac{\partial T}{\partial y} = \alpha\frac{\partial^2 T}{\partial y^2} + \tau\left[D_B\frac{\partial C}{\partial y}\frac{\partial T}{\partial y} + \frac{D_T}{T_\infty}\left(\frac{\partial T}{\partial y}\right)^2\right] \tag{3}$$

$$u\frac{\partial C}{\partial x} + v\frac{\partial C}{\partial y} = D_B\frac{\partial^2 C}{\partial y^2} + \frac{D_T}{T_\infty}\frac{\partial^2 T}{\partial y^2} \tag{4}$$

$$u\frac{\partial N}{\partial x} + v\frac{\partial N}{\partial y} + \frac{bWc}{C_\infty}\left[\frac{\partial}{\partial y}\left(N\frac{\partial C}{\partial y}\right)\right] = D_m\frac{\partial^2 N}{\partial y^2} \tag{5}$$

The boundary conditions can be set in the following form [14]:

$$u = U_w(x), v = 0, T = T_w, D_B\frac{\partial C}{\partial y} + \frac{D_T}{T_\infty}\frac{\partial T}{\partial y} = 0, N = N_w \text{ at } y = 0 \tag{6a}$$

$$u = U_\infty(x), T = T_\infty,\ C = C_\infty,\ N = N_\infty \text{ as } y \to \infty \tag{6b}$$

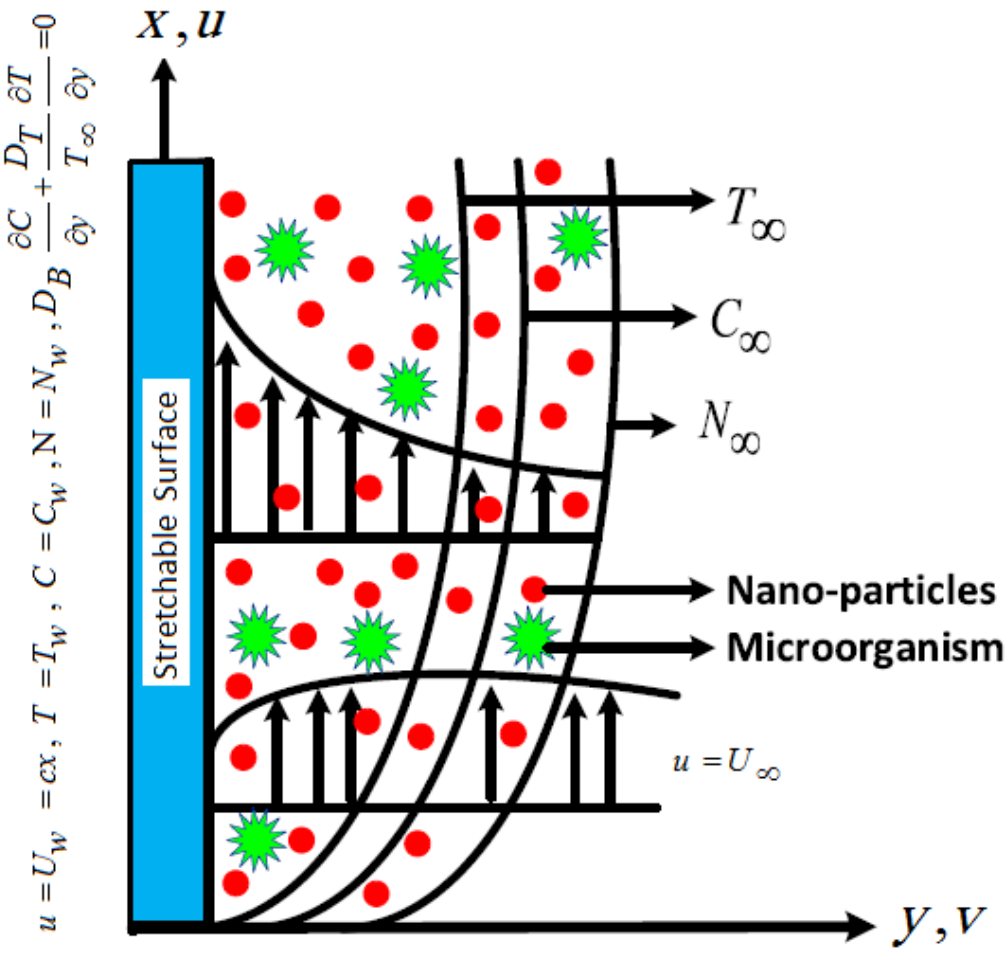

Figure 1. Schematic functionality of the flow.

In the present problem, we have ∂u/∂y > 0 when a/c > 1 (the ratio of free stream velocity and stretching velocity), which gives the shear stress where $\tau_{xy} = K(\partial u/\partial y)^n$. Here, K is the consistency coefficient and n is the power-law fluid. It is noted that, when n = 1, the fluid is Newtonian; when n < 1, the fluid is called pseudoplastic power-law fluid; and when n > 1, it is called dilatants power-law fluid.

Here (u, v) are the velocity components, along with the (x, y) directions. Here, T, C, and N are the fluid temperature, concentration, and density of motile microorganisms, respectively, and g is the gravitational acceleration. Wc denotes the maximum cell swimming speed, α stands for thermal diffusivity, β is the coefficient of thermal expansion, γ represents the average volume of a microorganism, ρ_f represents the density of the fluid, ρ_p denotes the density of the particles, ρ_m is the density of the microorganism, $\tau = (\rho c)_p/(\rho c)_f$ is the nanofluid heat capacity ratio, $(\rho c)_f$ is the heat capacity of the base fluid and $(\rho c)_p$ is the effective heat capacity of the nanoparticle material, Dn stands for diffusivity of the microorganisms, D_B represents the Brownian diffusion coefficient, and D_T stands for the thermophoretic diffusion coefficient of the microorganisms.

It is observed that the continuity equation is automatically determined by specifying the upgraded stream function, such that $u = (\partial\psi/\partial y)$, $v = -(\partial\psi/\partial x)$, and exhibits the following non-dimensional variables:

$$\theta = \frac{T-T_\infty}{T_w-T_\infty}, \phi = \frac{C-C_\infty}{C_\infty}, \chi = \frac{N-N_\infty}{N_w-N_\infty},$$
$$\psi = \left(\frac{K/\rho_f}{c^{1-2n}}\right)^{1/(n+1)} x^{2n/(n+1)} F(\eta),\ \eta = y\left(\frac{c^{2-n}}{K/\rho_f}\right)^{1/(n+1)} x^{(1-n)/(1+n)} \quad (7)$$

Equations (1)–(5) take the following non-dimensional form [8,9]:

$$nF''^{(n-1)}F''' + \frac{2n}{1+n}FF'' - F'^2 + \varepsilon^2 + \lambda\theta - Nr\phi - Rb\,\chi = 0 \tag{8}$$

$$\theta'' + \Pr\left(\frac{2n}{1+n}F\theta' + Nb\theta'\phi' + Nt\theta'^2\right) = 0 \tag{9}$$

$$\phi'' + Sc\frac{2n}{n+1}F\phi' + \frac{Nt}{Nb}\theta'' = 0 \tag{10}$$

$$\chi'' + Sb\frac{2n}{1+n}F\chi' - Pe\left(\phi\chi' + (\chi+\sigma)\phi''\right) = 0 \tag{11}$$

$$F'(0) = 1, F(0) = 0, \theta(0) = 1, Nb\phi'(0) + Nt\theta'(0) = 0, \chi(0) = 1 \tag{12a}$$

$$F'(\infty) = \varepsilon, \theta(\infty) = 0, \phi(\infty) = 0, \chi(\infty) = 0 \tag{12b}$$

where the prime denotes differentiation with respect to η and $\lambda = \frac{Gr_x}{\mathrm{Re}_x^2}$ is the dimensionless mixed convection parameter, $Nr = \frac{(\rho_p-\rho_f)C_\infty}{\rho_f\beta(T_w-T_\infty)(1-C_\infty)}$ stands for the buoyancy ratio parameter, $Gr_x = \frac{(1-C_\infty)\rho_f g\beta(T_w-T_\infty)}{(K/\rho_f)^2}$ is the local Grashof number, $\mathrm{Re}_x = \frac{(cx)^{2-n}x^n}{K/\rho_f}$ is the local Reynolds number, $Nb = \frac{\tau D_B C_\infty}{cx^2\mathrm{Re}_x^{-2/(n+1)}}$ is the Brownian motion parameter, $Nt = \frac{\tau D_T(T_w-T_\infty)}{T_\infty cx^2\mathrm{Re}_x^{-2/(n+1)}}$ is the thermophoresis parameter, $\Pr = \frac{cx^2}{\alpha}\mathrm{Re}_x^{-2/(n+1)}$ is the Prandtl number and $Sc = \frac{cx^2}{D_B}\mathrm{Re}_x^{-2/(n+1)}$ is the Schmidt number, $Rb = \frac{(N_w-N_\infty)\gamma(\rho_m-\rho_f)}{\rho_f\beta(T_w-T_\infty)(1-C_\infty)}$ is the bioconvection Rayleigh number, and $\varepsilon = a/c$ stands for the ratio of the velocity parameter. $Sb = \frac{cx^2\mathrm{Re}_x^{\frac{-2}{1+n}}}{D_m}$ denotes the bioconvection Schmidt number, $\sigma = \frac{N_\infty}{N_w-N_\infty}$ is the bioconvection constant, and $Pe = \frac{bWc}{D_m}$ represents the bioconvection Peclet number.

Various engineering quantities of interest like local skin friction C_f, the local Nusselt number N_{ux}, and the local density of the motile microorganisms' number N_{nx} are explored for the present nanofluid flow model. These quantities are defined as follows:

$$C_f = \frac{2\tau_w}{(cx)^2\rho_f};\ Nu_x = \frac{q_w x}{k_f(T_w - T_\infty)};\ Nn_x = \frac{q_n x}{D_n(T_w - T_\infty)} \tag{13}$$

For more clarification, the expressions of the shear stress τ_w, wall flux q_w (i.e., heat flux), and q_n (i.e., motile microorganisms density flux) are given as follows:

$$\tau_w = K\left(\frac{\partial u}{\partial y}\right)_{y=0};\ q_w = -k_f\left(\frac{\partial T}{\partial y}\right)_{y=0};\ q_n = -D_n\left(\frac{\partial N}{\partial y}\right)_{y=0} \tag{14}$$

By invoking the transformations of Equation (8), Equations (15) and (16) are reduced as follows:

$$\frac{1}{2}C_f\mathrm{Re}_x^{1/(1+n)} = (F''(0))^n;\ Nu_x\mathrm{Re}_x^{-1/(1+n)} = -\theta'(0);\ Nn_x\mathrm{Re}_x^{-1/(1+n)} = -\chi'(0) \tag{15}$$

3. Numerical Solution and Code Validation

Using MAPLE 22, Equations (8)–(11) subject to boundary conditions (12) were solved numerically. In order to solve boundary value issues numerically, this software, by default, employs a four-fifths order Runge–Kutta–Fehlberg approach. Its reliability and precision have been repeatedly demonstrated in numerous heat transfer articles. The unity coefficient of the term was changed to a continuation $(101 - 100\lambda)$, or $(10 - 9\lambda)$ was used in the dsolve command in order to speed convergence for all values of the governing parameters selected for this investigation. Without making this adjustment, MAPLE produces results that do not conform to the asymptotic values, but produces results that have a sharp angle at which

the axis intersects. The numerical solution to challenging ODE boundary value problems in Maple's help section contains more details on resolving the convergence challenges. Using a value of 8 for the similarity variable $\eta_{\max}$, the asymptotic boundary conditions from Equation (12a,b) were substituted as follows.

$$F'(8) = \varepsilon, \theta(8) = 0, \phi(8) = 0, \chi(8) = 0 \tag{16}$$

The selection of $\eta_{\max} = 8$ guaranteed that all numerical solutions appropriately approximated the asymptotic values. This is a crucial feature that is frequently missed in the literature on boundary layer fluxes.

To authenticate the model's validity, we have compared the skin friction values for several values ε in Tables 1–3, while Table 4 compares the heat transfer values with the existing literature. It exhibits good agreement for various parameters, indicating that our numerical solution is valid.

Table 1. Comparison of numerical values of $F''(0)$ at $\lambda = 0,\ n = 1$.

ε	Ishak et al. [10]	Khan and Rashad [25]	Present Results
0.1	−0.9694	−0.96939	−0.969386154
0.2	−0.9181	−0.91811	−0.918107089
0.5	−0.6673	−0.66726	−0.667263673
2	2.0175	2.017503	2.0175028007
3	4.7294	4.729282	11.751990603

Table 2. Comparison of $F''(0)$ for various values of Pr at $n = 1$ and $\lambda = Nr = 0$.

Pr	Wang [23]	Gorla and Sidawi [24]	Khan and Pop [8]	Present Results
0.07	0.0656	0.0656	0.0663	0.0659
0.2	0.1691	0.1691	0.1691	0.1690
0.7	0.4539	0.5349	0.4539	0.4539
2.0	0.9113	0.9113	0.9113	0.9113
7.0	1.8954	1.8905	1.8954	1.8954
20.0	3.3539	3.3539	3.3539	3.3539
70.0	6.4622	6.4622	6.4621	6.4622

Table 3. Comparison of $F''(0)$ for various values of n and a/c at $n = 1$ and $\lambda = Nr = 0$.

n	Mahapatra et al. [27]	Present Results	Mahapatra et al. [27]	Present Results
	ε = 1.1		ε = 1.5	
0.4	0.1035	0.1043	1.2019	1.2020
0.6	0.1193	0.1238	0.1691	1.0170
0.8	0.1407	0.14210	0.9434	0.9431
1.0	0.1643	0.16412	0.9095	0.9089
1.2	0.1888	0.18871	0.8937	0.8932
1.5	0.2257	0.22504	0.8853	0.8840

Table 4. Comparison of numerical values of $-\theta'(0)$ at $\lambda = \varepsilon = Nb = Nt = 0,\ n = 1$.

Pr	Khan et al. [28]	Present Results
0.7	0.4539	0.45445
2	0.9113	−0.91135
7	1.8954	−1.89540
20	3.3539	−3.35391

4. Results and Discussion

In this study, the mixed bioconvective stagnation-point flow of a power-law nanofluid over a stretchy sheet was computationally studied using the Runge–Kutta–Fehlberg method of the seventh order (RKF7) in conjunction with the shooting method. The influence of gyrotactic microorganisms at the surface is taken into account. Figure 2a shows the effects of the bioconvection Rayleigh number and buoyancy parameter on the dimensionless velocity, with all other parameters held constant. We notice that the dimensionless velocity increases significantly in the vicinity of the surface and then drops to the boundary layer edge with the Rayleigh number Rb. The dimensionless velocity overshoots at the region of the surface owing to the existence of buoyant forces. The Rayleigh number increases the buoyancy forces because of bioconvection, increasing the dimensionless velocity. The effects of mixed convection and velocity ratio parameters on the dimensionless velocity are presented in Figure 2b. The convergence rate depends upon the velocity ratio parameter. As the velocity ratio increases, the convergence rate increases. Within the hydrodynamic boundary layer, the mixed convection parameter also plays an important role. When the mixed convection parameter is increased, the dimensionless velocity increases.

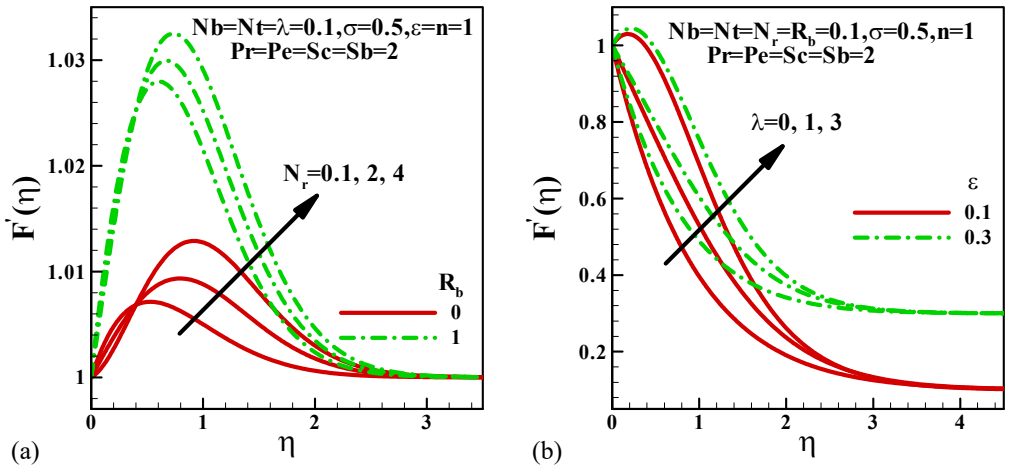

Figure 2. Variation of dimensionless velocity with (**a**) the buoyancy ratio parameter and bioconvection Rayleigh number and (**b**) the dimensionless mixed convection parameter and velocity ratio parameter.

The impacts of nanofluid parameters *Nb* and *Nt* are explained in Figure 3a. The Brownian motion parameter *Nb* keeps particles moving in a fluid. This keeps particles from settling, resulting in colloidal solutions that are more stable. It helps in enhancing the dimensionless velocity within the boundary layer. On the other side, the thermophoresis parameter generates a force due to temperature difference. Nanoparticles are transported towards the lower temperature zone by this force.

Consequently, the dimensionless velocity increases inside the boundary layer. In heat transfer, the bioconvection Schmidt number is equivalent to the Prandtl number. With a Schmidt number of one, momentum and mass transfer by diffusion are alike, and the velocity and concentration boundary layers are almost identical. An increasing bioconvection Schmidt number reduces the dimensionless velocity and hence the hydrodynamic boundary layer thickness, as shown in Figure 3b.

The effects of the thermophoresis parameter on the dimensionless temperature are presented in Figure 4 for several fluids. Thermophoresis is more important in a mixed convection process, where the flow is generated by the buoyancy force caused by a temperature differential. The nanoparticles move in the direction of a temperature drop, and decreasing the bulk density improves the heat transfer process. It is worth noting that nanoparticles transport thermal energy from high-temperature areas to lower-temperature areas. As a result, the thickness of the thermal boundary layer thickens as the thermophoresis parameter *Nt* increases. This fact is explained in Figure 4. The Prandtl number determines the

thickness of the thermal boundary layer. As the Prandtl number increases, the momentum diffusivity dominates the behavior and, as a result, the thickness of the thermal boundary layer decreases.

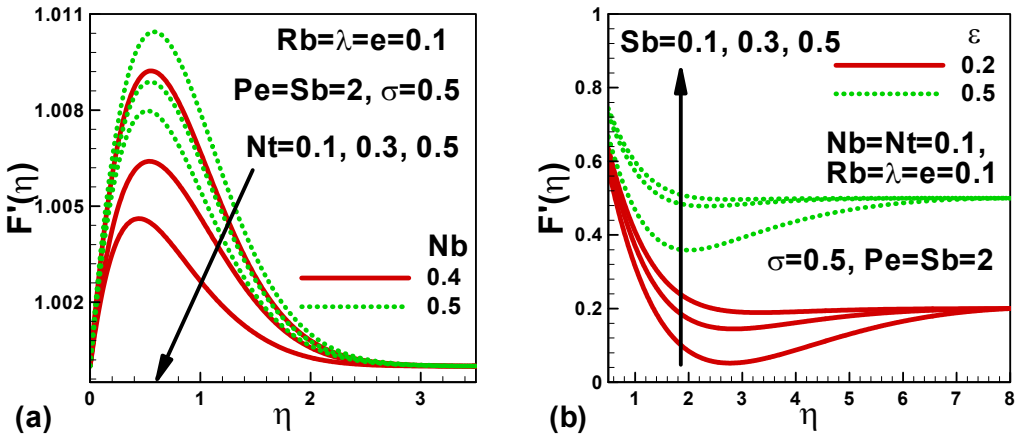

Figure 3. Variation of dimensionless velocity with (**a**) nanofluid parameters and (**b**) bioconvection Schmidt number.

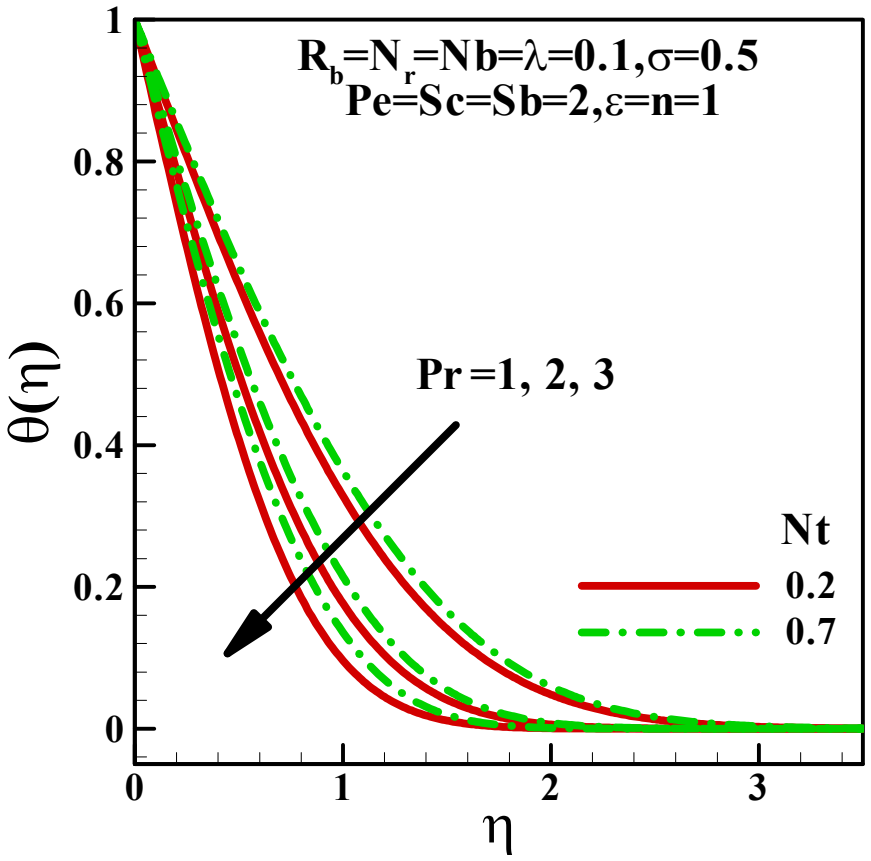

Figure 4. Variation in dimensionless temperature with the thermophoresis parameter for different fluids.

Figure 5a demonstrates the influence of nanofluid parameters on the dimensionless concentration at different thermophoresis parameters Nt = 0.4 and Nt = 0.5. The thermophoresis and Brownian processes cause the nanoparticle distribution to become non-uniform throughout the domain, as shown in Figure 5a. When the particle concentration is low and the Rayleigh number is low, the distribution of nanoparticles is more uniform.

Nanoparticle concentration rises when *Nt* increases because the thermophoresis parameter represents the movement of particles due to the temperature gradient.

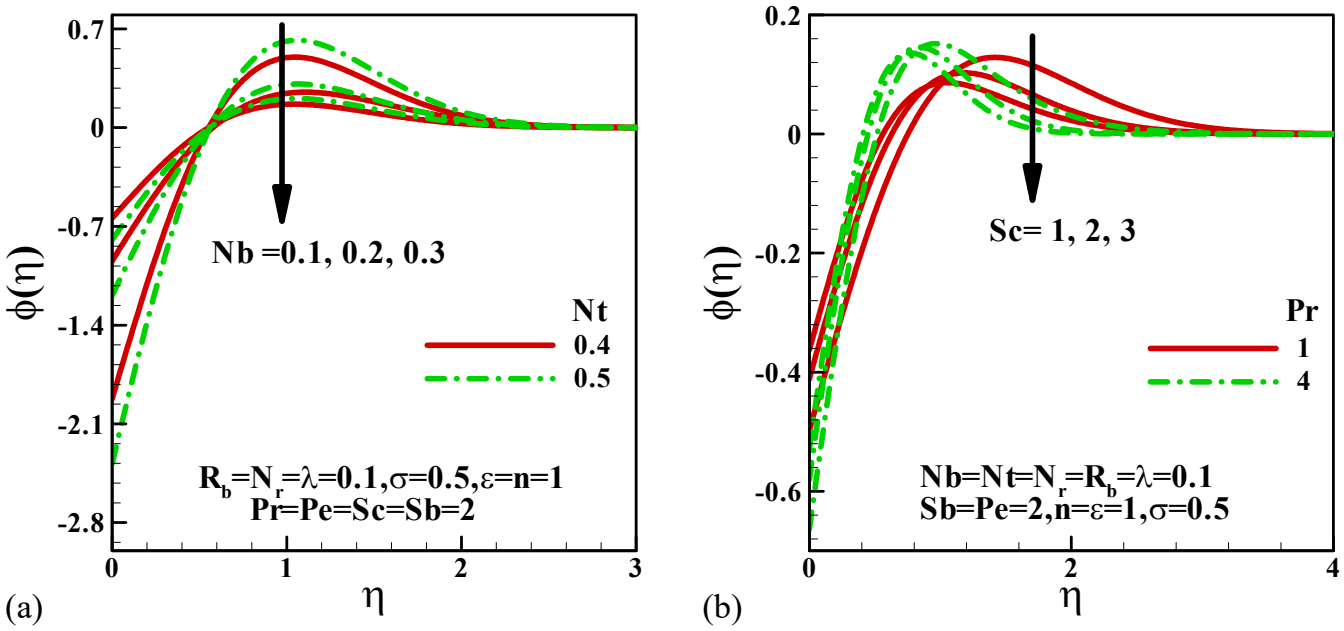

Figure 5. Variation in the dimensionless nanofluid concentration with (**a**) nanofluid parameters and (**b**) Schmidt number for different fluids.

Figure 5b depicts the influence of the Schmidt number Sc on the dimensionless concentration for several fluids. The dimensionless concentration overshoots near the surface and drops to zero, as observed. The reason is that the dimensionless velocity rises towards the surface before falling to zero. It is worth noting that, in the surface region, the dimensionless concentration rises with the Schmidt number. This is because the mass diffusivity diminishes, resulting in a lower concentration of nanoparticles. As a result, the concentration boundary layer thickness decreases as the Schmidt number Sc distance from the cone surface increases and increases as the Schmidt number *Nt* decreases. However, in the passively controlled model, it is assumed that there is no nanoparticle flux at the plate and that its particle fraction value adjusts accordingly. Thus, the passively controlled nanofluid model [26] can be used in practical applications. A numerical survey is then performed for all four profiles embodying the velocity, temperature, nanoparticle volumetric fraction, and density of motile microorganisms.

The effects of the bioconvection Schmidt number for different values of Peclet number are presented in Figure 6a. The large values of the Peclet number suggest an advectively dominated distribution, while a smaller value indicates a dispersed flow. As the Peclet number increases, the boundary layer thickness of motile microorganisms increases. Conversely, the bioconvection Schmidt number tends to suppress the boundary layer thickness. It is observed that the dimensionless motile microorganism density decreases with the bioconvection Schmidt number, but increases with the Peclet number. This can be attributed to the substantial decrease in mass diffusivity, which generates a lower concentration. Figure 6b illustrates the influence of the bioconvection constant for different values of the Brownian motion parameter. Nanoparticles are not self-propelled in a nanofluid. Brownian motion and the thermophoresis effect cause them to move. Motile microorganisms are mixed with a dilute suspension of nanoparticles to increase mass transfer and microscale mixing, as well as nanofluid stability in the flow. For this reason, the Brownian motion parameter tends to decrease the dimensionless microorganisms while the bioconvection constant tends to increase the microorganism's density.

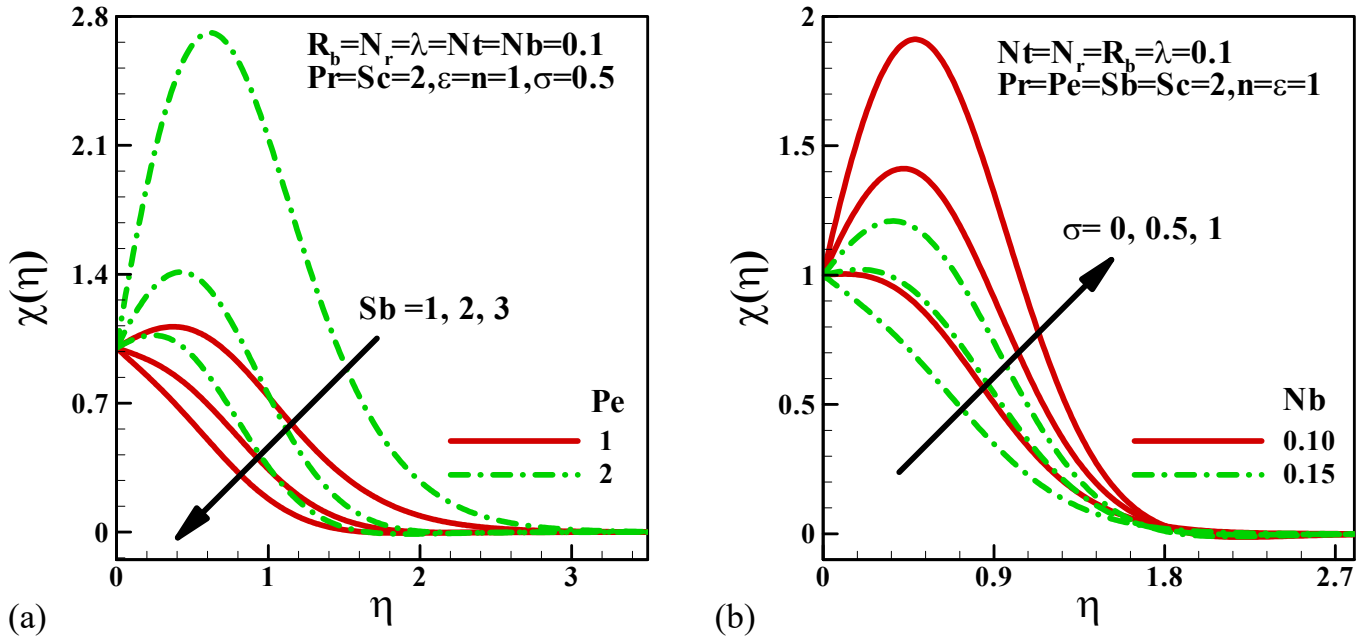

Figure 6. Variation of dimensionless motile micro-organism density with (**a**) the bioconvection Schmidt number with different Peclet numbers and (**b**) the bioconvection constant and Brownian motion parameter.

For several values of the bioconvection Rayleigh number and dimensionless mixed convection parameter, the variation in skin friction with the buoyancy ratio parameter is shown in Figure 7a. The skin friction is observed to rise with the bioconvection Rayleigh number and dimensionless mixed convection parameter, but decreases slightly with the buoyancy parameter. The skin friction is exceptionally high in the absence of the buoyancy effect and subsequently tends to decrease along with the buoyancy parameter. However, compared with buoyancy force convection, increasing the bioconvection Rayleigh number and dimensionless mixed convection parameter enhanced the convection heat. These results are anticipated; in the interim, heat is produced as a result of increased skin friction, resulting in the formation of a layer of hot fluid close to the surface. It is interesting to note that, as long as skin friction values are positive, we can see that drag force is imparted to the surface via the fluid. Figure 7b explains the effects of nanofluid parameters on the dimensionless heat transfer for different fluids. It is important to note that the Nusselt number decreases with both nanofluid parameters, but increases with the Prandtl number. It is commonly known that the Nusselt number represents the ratio of convective to conductive heat transfer; as a result, with more significant Nusselt numbers, heat convection predominates and the Nusselt number decreases as *Nb* and *Nt* increase.

The ratio of momentum diffusivity to mass diffusivity is known as the Schmidt number. In heat transmission, this is like the Prandtl number. When there is simultaneous momentum and mass transmission, this is used to characterize flows. The Sherwood number measures the efficacy of mass transfer at the surface. The variation in the Sherwood number with the Schmidt number is depicted in Figure 8a for different values of the thermophoresis parameter and Brownian number. It is perceived that the Sherwood number increases significantly with the Schmidt number and Brownian motion parameter. However, the thermophoresis parameter tends to reduce the Sherwood number.

The variation in the dimensionless local density number of the motile microorganisms with bioconvection parameters is depicted in Figure 8b. The motile microorganism mass transfer rate is significantly increased when the bioconvection Schmidt number increases. The bioconvection Peclet number and bioconvection constant reduce the rate of motile microorganism mass transfer. This is because Pe is directly related to *Wc* (maximum cell

swimming speed) and inversely proportional to D_m (the diffusivity of microorganisms). As a result, larger Pe values diminish microorganism speed and reduce microorganism diffusivity. This will result in lower microorganism concentrations in the border layer and a higher rate of motile micro-organism mass transfer.

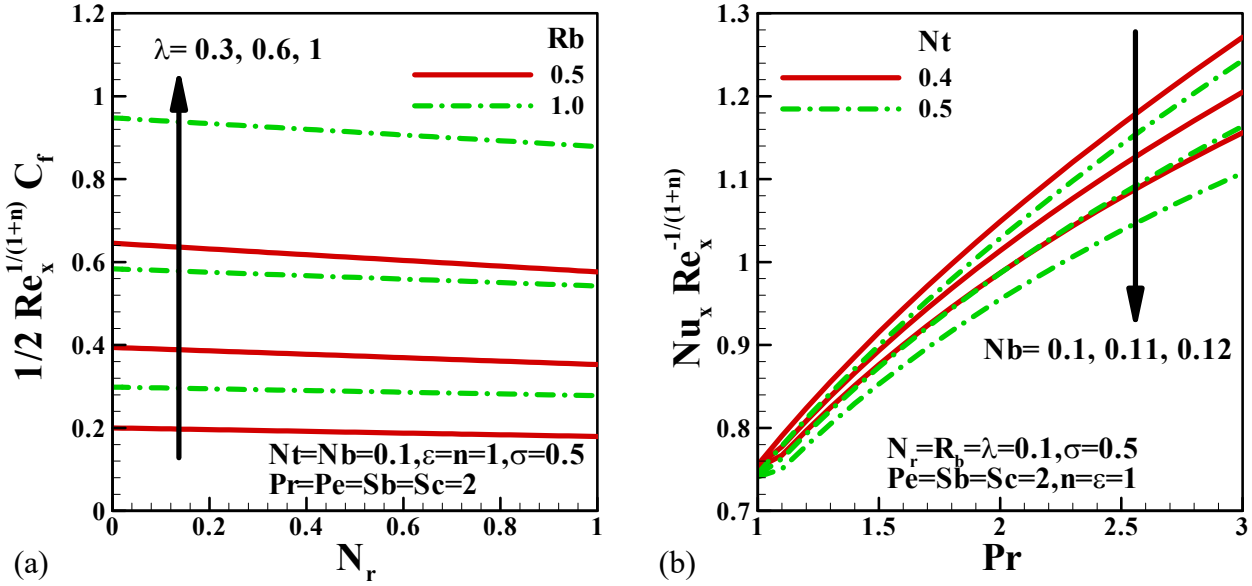

Figure 7. Variation in skin friction with (**a**) buoyancy ratio parameters for different values of bioconvection Rayleigh number and dimensionless mixed convection parameter and (**b**) variation in the Nusselt number with the Prandtl number for different values of nanofluid parameters.

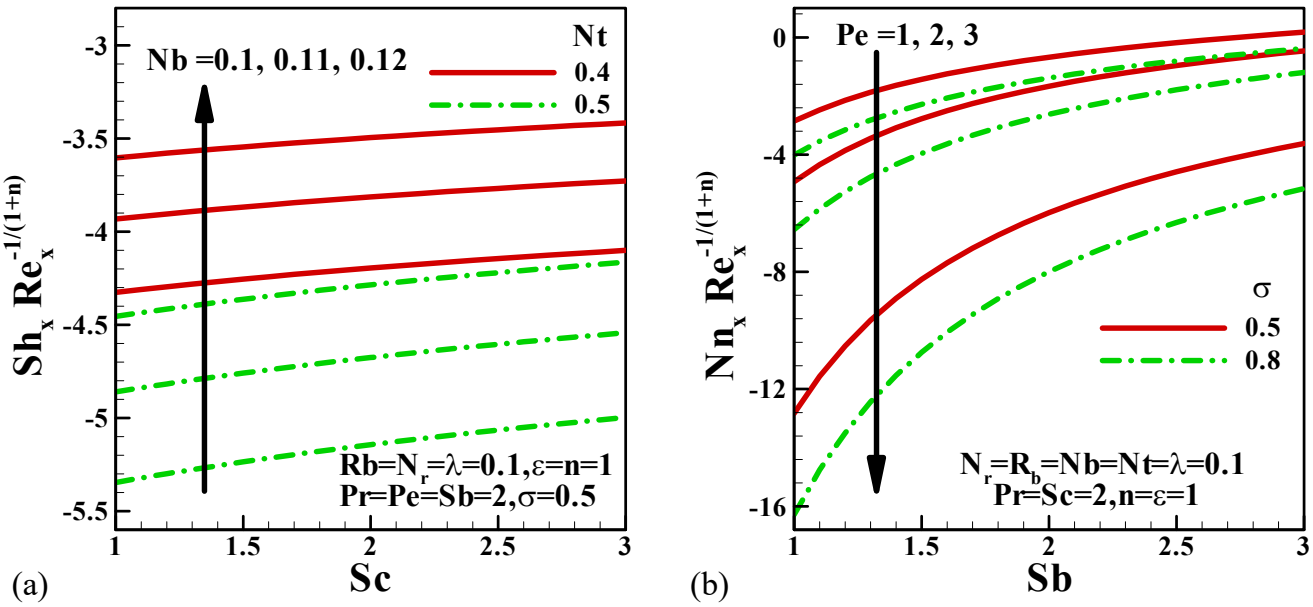

Figure 8. (**a**) Variation in the Sherwood number with the Schmidt number for different nanofluid parameters and (**b**) variation in the density number of the motile microorganisms.

5. Conclusions

The mixed bioconvective flow of water-based nanofluid containing micro-organisms is investigated numerically using a Runge-Kutta–Fehlberg method of the seventh order (RKF7) coupled with a shooting method. The effects of bioconvection and nanofluid parameters on the dimensionless variables and quantities of interest are investigated numerically. The results are presented graphically and are compared with the existing data.

In the RKF7 method, the following are the primary conclusions that can be deduced from the study:

- Besides the bioconvection Schmidt number, all other parameters enhance the dimensionless velocity inside the boundary layer.
- Thermal boundary layer thickness decreases with the increasing Prandtl number.
- The nanofluid parameters generate non-uniform nanoparticle distribution throughout the domain.
- Dimensionless motile microbe density decreases as the bio-convection Schmidt number rises, but rises when the Peclet number falls.
- Skin friction is slightly reduced by the buoyancy parameter, but is slightly increased by the dimensionless mixed convection parameter and the bioconvection Rayleigh number.
- Nanofluid parameters reduce the Nusselt number, while the Prandtl number enhances it.
- Schmidt number and Brownian motion parameter both significantly boost the Sherwood number. Thermophoresis, on the other hand, tends to lower the Sherwood number.
- The bioconvection Peclet number and bioconvection constant contribute to slowing down the rate of mass transfer in motile microorganisms.

Author Contributions: All authors contributed equally. All authors have read and agreed to the published version of the manuscript.

Funding: This research received no external funding.

Data Availability Statement: Data are available upon request.

Conflicts of Interest: The authors declare no conflict of interest.

Nomenclature

a and c	positive constants
C	concentration
C_f	local skin-friction coefficient
Dn	diffusivity of the microorganisms
D_B	Brownian diffusion coefficient
D_T	thermophoretic diffusion coefficient of the microorganisms
F'	dimensionless velocity
g	gravitational acceleration
Gr_x	local Grashof number
Sb	bioconvection Schmidt number
Sc	Schmidt number
K	consistency coefficient
k_f	thermal conductivity
N	density of motile microorganisms
n	power-law fluid
Nb	Brownian motion number
Nr	buoyancy ratio parameter
Nt	thermophoresis number
Nu_x	Nusselt number
Nn_x	density number
Pe	bioconvectionPéclet number
Pr	Prandtl number
q	wall heat flux
Rb	bioconvection Rayleigh number
Re_x	local Reynolds number
T	temperature
u and v	dimensionless velocity component in the x-direction

$U_w(x)$	stretching velocity
$U_\infty(x)$	free stream velocity
w_c	maximum cell swimming speed
x	streamwise coordinate
y	transverse coordinate
Greek Symbols	
α	thermal diffusivity
β	coefficient of thermal expansion
γ	average volume of a microorganism
σ	bioconvection constant
η	pseudo-similarity variable
θ	dimensionless temperature
φ	nanoparticle volume fraction
ψ	non-dimensional stream function
λ	mixed convection parameter
ε	ratio of velocity parameter
χ	dimensionless density of motile microorganisms
μ	dynamic viscosity
ν	kinematic viscosity
ρ_f	density of the fluid
$\rho_{f\infty}$	density of the base fluid
ρ_p	density of the particles
$\rho_{m\infty}$	density of the microorganism
$(\rho c)_f$	heat capacity of the fluid
$(\rho c)_p$	effective heat capacity of the nanoparticle material
ρ	density
Subscripts	
w	condition at the wall
∞	condition at infinity

References

1. Choi, S.U.S. Enhancing thermal conductivity of fluids with nanoparticles. In Proceedings of the 1995 ASME International Mechanical Engineering Congress and Exposition, San Francisco, CA, USA, 12–17 November 1995; pp. 99–105.
2. Das, K.; Putra, N.; Thiesen, P.; Roetzel, W. Temperature dependence of thermal conductivity enhancement for nanofluid. *J. Heat Transf.* **2003**, *125*, 567–574. [CrossRef]
3. Gorla, R.S.R.; El-Kabeir, S.M.M.; Rashad, A.M. Heat transfer in the boundary layer on a stretching circular cylinder in a nanofluid. *J. Thermophys. Heat Transf.* **2011**, *25*, 183–186. [CrossRef]
4. Chamkha, A.J.; Rashad, A.M. Natural convection from a vertical permeable cone in nanofluid saturated porous media for uniform heat and nanoparticles volume fraction fluxes. *Int. J. Numer. Methods Heat Fluid Flow* **2012**, *22*, 1073–1085. [CrossRef]
5. Chamkha, A.J.; Rashad, M.; Gorla, R.S.R. Non-Similar Solutions for Mixed Convection along with a Wedge Embedded in a Porous Medium Saturated by a Non-Newtonian Nanofluid: Natural Convection Dominated Regime. *Int. J. Numer. Methods Heat Fluid Flow* **2014**, *24*, 1471–1786. [CrossRef]
6. Buongiorno, J. Convective transport in nanofluids. *ASME J. Heat Transf.* **2006**, *128*, 240–250. [CrossRef]
7. Khan, W.A.; Rashad, A.M.; Abdou, M.M.M.; Tlili, I. Natural Bioconvection Flow of A Nanofluid Containing Gyrotactic Microorganisms About A Truncated Cone. *Eur. J. Mech./B Fluids* **2019**, *75*, 133–142. [CrossRef]
8. Chamkha, A.J.; Nabwey, H.A.; Abdelrahman, Z.M.A.; Rashad, A.M. Mixed Bioconvective Flow Over a Wedge in Porous Media Drenched with a Nanofluid. *J. Nanofluids* **2020**, *9*, 24–35. [CrossRef]
9. Nabwey, H.A.; El-Kabeir, S.M.M.; Rashad, A.M.; Abdou, M.M.M. Viscous Dissipation and Joule Heating Effects on MHD Bioconvection Flow of a Nanofluid Containing Gyrotactic Microorganisms over a Vertical Isothermal Cone. *J. Nanofluids* **2020**, *9*, 242–255. [CrossRef]
10. Nabwey, H.A.; El-Kabeir, S.M.M.; Rashad, A.M.; Abdou, M.M.M. Gyrotactic Microorganisms Mixed Convection Flow of Nanofluid over a Vertically Surfaced Saturated Porous Media. *Alex. Eng. J.* **2021**, *61*, 1804–1822. [CrossRef]
11. Irvine, T.F.; Karni, J. Non-Newtonian fluid flow and heat transfer. In *Handbook of Single-Phase Convective Heat Transfer*; Kakac, S., Shah, R.K., Aung, W., Eds.; Wiley: New York, NY, USA, 1987; pp. 20.1–20.57.
12. Schowalter, W.R. The application of boundary-layer theory to power-law pseudoplastic fluids: Similar solutions. *AICHE J.* **1960**, *6*, 24–28. [CrossRef]
13. Acrivos, A.; Shah, M.J.; Petersen, E.E. Momentum and heat transfer in laminar boundary layer flows of non-Newtonian fluids past external surfaces. *AICHE J.* **1960**, *6*, 312–318. [CrossRef]

14. Rashad, A.M.; EL-Hakiem, M.A.; Abdou, M.M.M. Natural convection boundary layer of a non-Newtonian fluid about a permeable vertical cone embedded in a porous medium saturated with a nanofluid. *Comput. Math. Appl.* **2011**, *62*, 3140–3151. [CrossRef]
15. Rashad, A.M.; Chamkha, A.J.; Abdou, M.M.M. Mixed Convection Flow Of Non-Newtonian Fluid From Vertical Surface Saturated In A Porous Medium Filled with A Nanofluid. *J. Appl. Fluid Mech.* **2013**, *6*, 301–309.
16. Chamkha, A.J.; Abbasbandy, S.; Rashad, A.M. Non-Darcy Natural Convection Flow of a Non-Newtonian Nanofluid over a Cone Saturated in a Porous Medium with Uniform Heat and Volume Fraction Fluxes. *Int. J. Numer. Methods Heat Fluid Flow* **2015**, *25*, 422–437. [CrossRef]
17. Nabwey, H.A.; Boumazgour, M.; Rashad, A.M. Group Method Analysis Of Mixed Convection Stagnation-Point Flow of Non-Newtonian Nanofluid over a Vertical Stretching Surface. *Indian J. Phys.* **2017**, *91*, 731–742. [CrossRef]
18. Platt, J.R. Bioconvection Patterns in Cultures of Free-Swimming Organisms. *Science* **1961**, *133*, 1766–1767. [CrossRef]
19. Kuznetsov, A.V.; Avramenko, A.A. Effect of small particles on the stability of bioconvection in a suspension of gyrotactic microorganisms in a layer of finite depth. *Int. Commun. Heat Mass Transf.* **2004**, *31*, 1–10. [CrossRef]
20. Kuznetsov, A.V. The onset of nanofluidbioconvection in a suspension containing both nanoparticles and gyrotactic microorganisms. *Int. Commun. Heat Mass Transf.* **2010**, *37*, 1421–1425. [CrossRef]
21. Waqas, H.; Khan, S.U.; Hassan, M.; Bhatti, M.M.; Imran, M. Analysis of the bioconvection flow of modified second-grade nanofluid containing gyrotactic microorganisms and nanoparticles. *J. Mol. Liq.* **2019**, *291*, 111231. [CrossRef]
22. Khan, W.A.; Uddin, M.J.; Ismail, A.I. Free convection of non-Newtonian nanofluids in porous media with gyrotactic microorganisms. *Transp. Porous Media* **2013**, *97*, 241–252. [CrossRef]
23. Khan, W.A.; Rashad, A.M. Combined effects of radiation and chemical reaction on heat and mass transfer by MHD stagnation-point flow of a Micropolar fluid towards a stretching surface. *J. Niger. Math. Soc.* **2017**, *36*, 219–238.
24. Beg, O.A.; Uddin, M.J.; Khan, W.A. Bioconvective Non-Newtonian Nanofluid Transport in Porous Media Containing Micro-Organisms in a Moving Free Stream. *J. Mech. Med. Biol.* **2015**, *15*, 5. [CrossRef]
25. Ishak, A.; Nazar, R.; Pop, I. Mixed convection boundary layers in the stagnation point flow toward a stretching vertical sheet. *Meccanica* **2006**, *41*, 509–518. [CrossRef]
26. Kuznetsov, A.V.; Nield, D.A. Natural convective boundary-layer flow of a nanofluid past a vertical plate: A revised model. *Int. J. Therm. Sci.* **2014**, *77*, 126–129. [CrossRef]
27. Mahapatra, T.R.; Nandy, S.K.; Gupta, A.S. Magnetohydrodynamic stagnation-point flow of a power-law fluid towards a stretching surface. *Int. J. Non-Linear Mech.* **2009**, *44*, 123–128. [CrossRef]
28. Khan, M.; Malik, R.; Munir, A.; Khan, W.A. Flow and heat transfer to Siskonanofluid over a nonlinear stretching sheet. *PLoS ONE* **2015**, *10*, e0125683.